PIV and CFD measurements of internal velocity in a forming drop in a liquid-liquid system

Timgren, Anna; Trägårdh, Gun; Trägårdh, Christian

Published in:
7th International Symposium on Particle Image Velocimetry

2007

PIV and CFD measurements of internal velocity in a forming drop in a liquid-liquid system

Anna Timgren, Gun Trägårdh and Christian Trägårdh

Lund University, Department of Food Technology, Engineering and Nutrition

P.O. Box 124, SE-221 00 Lund, Sweden

E-mail: Anna.Timgren@food.lth.se

Tel: +46 46 222 9817

Abstract A PIV method has been used to determine the internal motion in an oil drop during formation and to validate a numerical simulation of the drop formation process. The PIV system included a microscope attached to the camera, which gave a focal depth of 50 µm and a possibility to measure the velocity in the centre cross section of the drop. Oil was forced through a capillary with a diameter of 200 µm into a channel with a cross-flowing continuous phase that induced a shear at the interface of the forming drop, which resulted in a rotational motion inside the drop. The angular velocity in the drop reached a maximum after 1/4 of the drop formation time and approached a steady state before drop detachment when a neck was formed above the capillary opening. The velocity of oil out of the capillary was also investigated. A clear dependence on the pressure inside the forming drop was obtained.

1 Introduction

A better understanding of drop formation and detachment from a pore or capillary can be used to improve many industrial processes, including chemical reactions, and combustion and emulsification processes. Drops can, for instance, be formed in processes involving microchannels, a nozzle or the pores in a membrane. Although the drops thus formed commonly disperse into another immiscible liquid flowing past the forming drop, few studies focus on liquid drop formation in a cross-flowing immiscible liquid, as was the case in this study.

The creation of drops from a capillary involves two main steps: (1) drop formation, in which the dispersed phase is forced out of the capillary, and the drop grows at the capillary opening, and (2) detachment, when the drop forms a neck, detaches from the dispersed phase and moves with the surrounding continuous phase. Two possible mechanisms are suggested in the literature for the detachment step: *spontaneous transformed based* droplet formation, in which the drops detach because of the minimization of free energy (Sugiura et al. 2001, Yasuno et al. 2002, Rayner et al. 2004), and *shear-induced* droplet formation, in which the detachment is influenced by the cross-flow of the continuous phase (Schröder et al. 1998, Joscelyne and Trägårdh 1999, Wang et al. 2000, Kobayashi et al. 2002, Yasuno et al. 2002). In shear-induced formation, detachment is explained by the fact that the continuous phase has considerable viscous effects when flowing tangentially to the capillary opening. The shear stress and pressure gradient resulting from the cross-flow cause a drag and a lift force, which promote drop detachment.

Experimental numerical studies have shown that motion arise inside a liquid sphere when affected by a cross-flow. As the continuous phase shears the interface of a growing drop, the dispersed phase inside the forming drop starts to rotate and forms a vortex (Timgren et al.). Hill established long ago the shear effects of a gas cross-flow on the internal motion in a droplet (Hill, 1894). More recent experimental and numerical studies of a free liquid sphere in an air stream

show that the internal motion in the drop is dependent on the direction of the surrounding air stream (Megaridis et al. 1994). Antar and El-Shaarawi (2002a, 2002b and 2004) have presented several numerical studies on the boundary-layer flow around a liquid sphere in an external flow of air, and the effects of viscosity ratio, internal motion and Reynolds number on the local shear stress. They found that shear stress increased with increasing viscosity ratio and spin parameter, and decreasing Reynolds number. The involvement of this internal motion in the drop detachment process remains, however, unexplained. The PIV method can be used to visualizing and measuring the motion and velocity profile inside a drop (Timgren et al.). This provides new insight into the drop formation and detachment process. PIV has also been used for other applications involving a two-phase system consisting of oil and water with matching refractive indices (Mohamed-Kassim and Longmire, 2003; 2004; Milosevic and Longmire, 2002; Augier et al., 2003).

The formation and detachment of a liquid drop in an immiscible liquid have been modelled with computational fluid dynamics (CFD) by a number of researchers. Kobayashi et al. (2004 and 2006) investigated the impact of pore geometry and the flow of the dispersed phase on the necking and size of droplets (30-70 µm in diameter) formed in a stagnant continuous phase, and found that detachment occurs inside an elliptic pore if the aspect ratio exceeds 3.5. In order to improve the design of a membrane for membrane emulsification Abrahamse et al. (2001) simulated drop formation in a 5 µm cylindrical pore in laminar cross-flow. They found that the pressure drop over the pore and the velocity in the pore decreased when a neck was formed on the growing droplet and the drop detached above the pore opening. Drops formed from larger nozzles, 0.5-4 mm, have been simulated by, among others, Ohta et al. (1995 and 2003) and Schönfeld and Rensink (2003). However, no one has, as far as we know, focused on the internal motion in a forming drop, induced by the cross-flow of a continuous phase during drop formation from a capillary with a diameter of 200 µm as was studied here.

The aim of this work was twofold. Firstly, the effect of the flow of the continuous and the dispersed phases on the internal motion and angular velocity in a drop when this is formed at a single circular pore in a laminar cross-flow was determined. For this purpose a PIV method that is able to measure velocities inside an oil drop was used. Secondly, the results from the PIV measurements were compared to a CFD simulation where a commercial CFD code and the volume of fluid (VOF) method were used.

2 Materials and methods

Fig. 1 shows a sketch of the experimental set-up for the flow system used in the study. The experiments were performed in a rectangular steel channel with a glass window to allow imaging, and a PMMA (polymethyl methacrylate) window for the laser illumination. The channel was 20 mm in width, 5 mm in height and 500 mm long to achieve a laminar profile in the measurement region. The continuous phase was pumped through the channel and the dispersed phase was kept in a container and forced by a constant overpressure through a glass capillary with an inner diameter of 200 µm and a length of 15 mm. The continuous phase consisted of a mixture of water and glycerol with the same refractive index (1.401) as the silicon oil that was used as the dispersed phase. The density was 1130 and 960 kg/m^3 and the viscosity was 6.7 and 48 mPa s for the continuous and dispersed phase, respectively. The measured surface tension was 29.5 mN/m.

The oil in the capillary flowed into the centre at the bottom of the measurement region of the channel and drops were formed continuously. The mean velocity in the cross-flow was 0.07 m/s and the applied pressure on the oil phase was 90 kPa, which resulted in a drop formation time of approximately 0.5 drops/s.

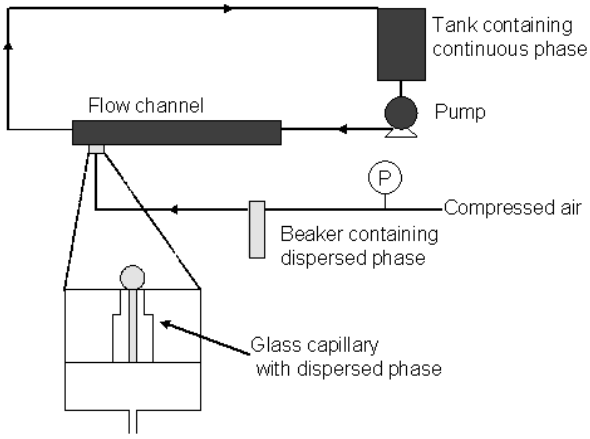

Fig. 1. Sketch of the experimental set-up of the flow system showing an enlargement of the region including the glass capillary

Rhodamine-B-labelled melamine resin particles (microParticles GmbH) with a diameter of 1.05 µm (±0.040 µm) were used as seeding particles. This particle size was chosen because the image spot of the light scattered by these particles corresponds to 1-2 pixels, which is the optimum particle-image diameter according to Westerweel (2000). The estimated response time of these particles is 10 ns and, compared to the characteristic time of the flow, which is over 5 µs, it can be assumed that the particles follow the motion of the fluids with respect to Stokes' number (Crowe et al., 1998). The particles emit light at a wavelength of approximately 560 nm, with an emission peak at 584 nm. The concentration of particles was 3×10^{10} particles per litre fluid, which gives a seeding density of at least 10 particles per interrogation area with a size of 32×32 pixels, and an estimated acceptable focal depth of 50 µm.

The visualisation system is illustrated in Fig. 2. The particles in the flow system were illuminated by a Nd:YAG double-pulsed laser (New Wave Research) with a wavelength of 532 nm and a pulse width of about 5 ns. The laser beam was transformed into a sheet using an optical system and directed through the PMMA window of the channel. It was ensured that the light sheets originating from the two laser beams had identical intensity and position, and were parallel to the long axis of the channel. The CCD camera (Flowmaster 3, LaVision GmbH) used was attached to a microscope (BX30, Olympus) with a ×0.5 magnification adaptor inserted between the microscope and the camera and a long-pass filter with a cut-off of 570 nm (03 FCG 498, Melles Griot). A long working distance objective (LMPlanFL x5, Olympus) was used with the microscope, which gives a total magnification of ×2.5 and an acceptable focal depth of approximately 50 µm. The camera has a matrix of 1280×1024 pixels and a 12-bit intensity resolution. The PIV system was controlled by a LaVision hardware timing unit which triggered the measurements. Double frame, double exposure was used for the velocity measurements in the oil drop and the time interval between the two pulses was 1000 µs.

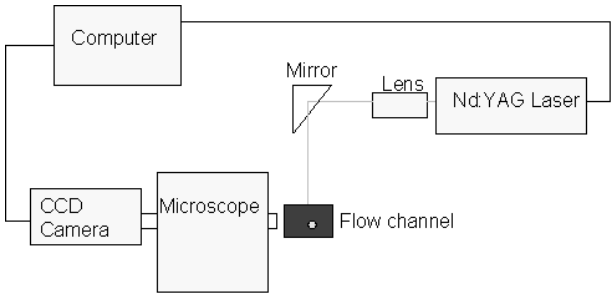

Fig. 2. Sketch of the experimental set-up of the visualisation system

DaVis 6.2 software (LaVision GmbH) was used to process and evaluate the images. The velocity vectors inside the oil drops were calculated using the cross-correlation algorithm in a rectangle that included the drop. The rectangles were divided into IAs of 32×32 or 16×16 pixels with an overlap of 50%, and processed using a multi-pass algorithm with decreasingly smaller IAs, resulting in a spatial resolution down to 21.3 µm. The images were post-processed using a local median filter (Westerweel, 1993) with an allowed range of deviation of 1.3 times the root mean square of the neighbouring vectors.

The CFD software Fluent 6.2.16 (Fluent Inc., 2005) was used to simulate the formation and detachment of a drop into a cross-flowing continuous phase. Fluent uses a control-volume-based technique to convert the governing equations into algebraic equations that can then be solved numerically. The governing equation used was the mass conservation equation for each phase and the momentum equation. The three-dimensional geometry of the channel and capillary, and the meshes of the fluid volumes were generated using Gambit 2.2.30 (Fluent Inc., 2004). The capillary, which has a circular cross sectional diameter of 200 µm and a length of 15 mm, is connected to a channel with a length, height and width of 4×5×4 mm, respectively, see Fig. 3.

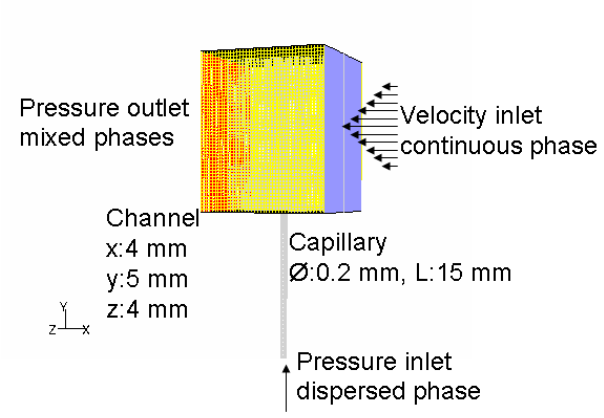

Fig. 3. Geometry and boundary settings of the model

The Cartesian coordinates have their origin at the centre of the capillary opening. The mesh is composed primarily of hexahedral elements, but includes wedge-shaped elements where appropriate. Since a Cooper type scheme was used in Gambit, the volume mesh is based on specified source faces and the capillary opening is one of these faces, which results in a finer mesh in the channel just above the capillary. A hexahedral mesh was selected on the grounds that the calculations of surface tension effects are more accurate with this mesh than with a triangular or tetrahedral mesh. Mesh refinement was adopted in Fluent in order to increase the resolution of the drop formation area. A grid convergence study

has been carried out previously (Timgren et al. 2007). Silicon oil was assumed to be the dispersed phase and a mixture of water and glycerol the continuous phase just as in the experimental trials and the fluids are assumed to be incompressible and isothermal. The volume of fluid (VOF) method was used to track the interface between the oil drop and the continuous phase. The VOF model is a surface-tracking technique that is useful when studying the position of the interface between two immiscible fluids. A single set of momentum equations is shared by the fluids, and the volume fraction of each of the fluids in each computational cell is tracked throughout the domain. The VOF model uses phase averaging to define the amount of continuous and dispersed phase in each cell. A variable, α, was defined as:

$\alpha = 1 \Rightarrow$ when the cell is 100% filled with continuous phase
$\alpha = 0 \Rightarrow$ when the cell is 100% filled with dispersed phase
$0 < \alpha < 1 \Rightarrow$ when the cell contains an interface between the two phases

The boundary conditions are illustrated in Fig. 3 and described below with the following initial conditions.

- The operating pressure was set to atmospheric pressure.
- The entrance of the channel was defined as velocity inlet with a user-defined function (UDF) as initial condition. The UDF is a laminar velocity profile in the y-direction with a maximum velocity ($U_{c,max}$) of 0.11 m/s at y=2.5 mm.
- The entrance of the capillary was defined as pressure inlet with a constant gauge pressure on the disperse phase. The gauge pressure was set to 7000 Pa.
- The outflow of the channel was defined as pressure outlet with zero gauge pressure.
- The side walls of the channel were defined as symmetry since the real channel used in the experimental study had a width of 20 mm. Thus, the velocity at these walls follows the velocity profile defined at the channel entrance, which can be assumed to be correct since the axial velocity profile in the horizontal plane is flat in the rectangular channel used.
- All other walls are assumed to be stationary with a no-slip boundary condition, and a contact angle of 179°.
- The time step was set to 10^{-5} s.

3 Results and discussion

The results of the PIV measurement show the ability of this method to study the velocity inside a forming oil drop with a final diameter of about 1 mm. The objective used with the microscope has a working distance of 22.5 mm and an acceptable focal depth of 50 µm, which has the capacity to focus at the centre of the drop through the surrounding continuous phase when the refractive indices of the two phases match. Fig. 4, 5 and 6 show the velocity vectors inside the drop measured by the PIV technique (Fig. 4a, 5a and 6a) and numerically simulated with CFD (Fig. 4b, 5b and 6b). The total drop formation time was approximately 2.25 seconds. Fig. 4, 5 and 6 show the vectors after 0.18, 0.63 and 2.16 s of the drop formation time, respectively. The velocity field in the centre cross section of a forming drop can be compared to a large vortex. This rotational motion was

obviously induced by the shear arising from the cross-flow of the continuous phase. However, the accelerated fluid of oil out of the capillary was also affecting the motion inside the forming drop. The velocity fields from the CFD simulation by Abrahamse et al. (2001) show a less obvious vortex inside the drop when this is formed from a capillary with a diameter of 5 µm. This is mainly because the velocity in the capillary was relatively high and therefore affects the motion inside the drop to a greater extent than in the present study.

A good correlation can be seen in the illustrated velocity vector fields between the PIV experiment and the CFD simulation in Fig. 4, 5 and 6. However, there are some misalignments in the position of the vortex centre and in the velocity vectors near the capillary opening. The difference above the capillary opening can be due to the reflexes from the bottom of the channel during the PIV experiments, which will disturb the calculation of the vectors. A minor deviation between the centre of the drop and the focus of the microscope can be another reason. This can also be the cause of the difference in the position of the vortex centre. This will have a greater effect when the drop is small (Fig. 4) since the focal depth then is 1/10 of the drop diameter compared to 1/25 in Fig. 6 where the vortex position correlates better. The misalignment in vortex position may also be influenced by the motion in the remaining oil after detachment.

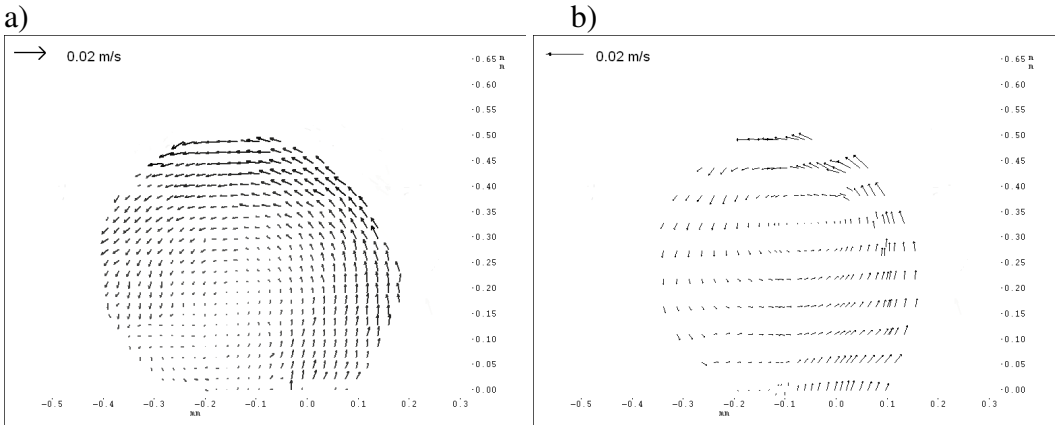

Fig. 4. Velocity vectors inside an oil drop formed in a cross-flow of continuous phase from right to left after 0.18 s of the drop formation time. a) PIV measurement with 16×16 px IAs and b) CFD simulation.

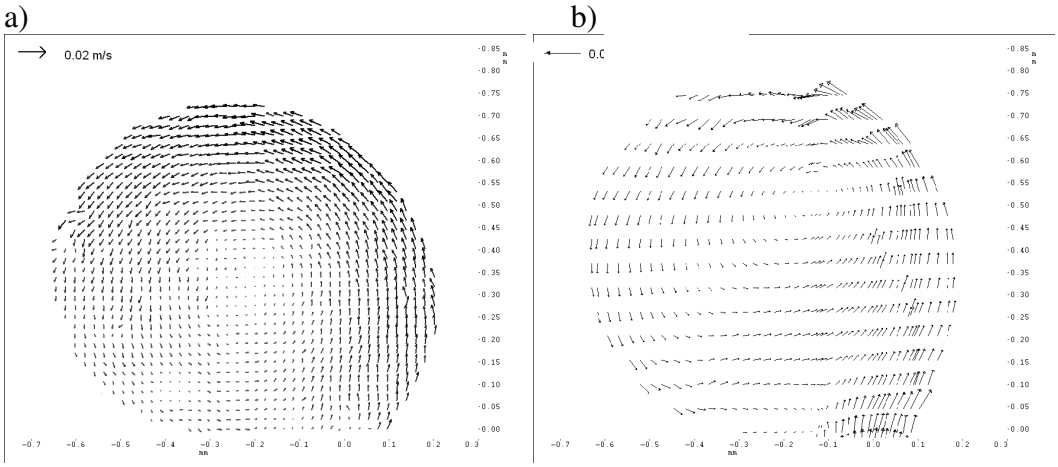

Fig. 5. Velocity vectors inside an oil drop formed in a cross-flow of continuous phase from right to left after 0.63 s of the drop formation time. a) PIV measurement with 16×16 px IAs and b) CFD simulation.

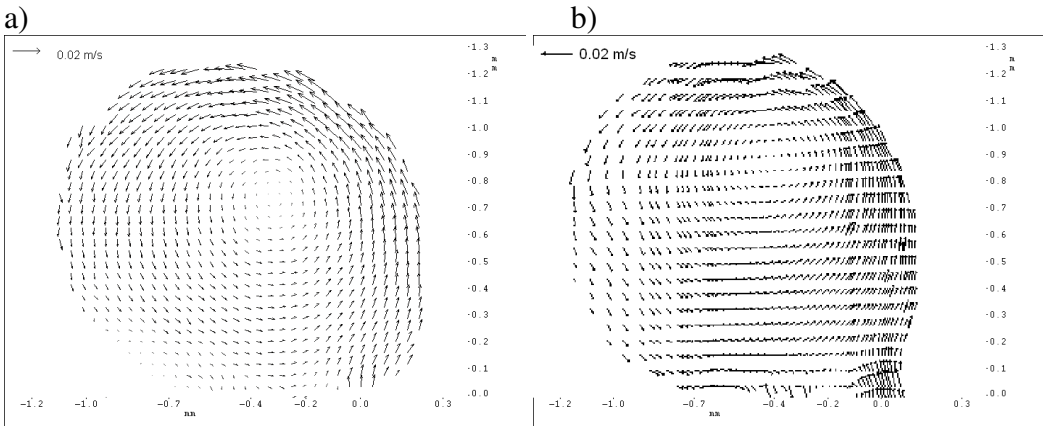

Fig. 6. Velocity vectors inside an oil drop formed in a cross-flow of continuous phase from right to left after 2.16 s of the drop formation time. a) PIV measurement with 32×32 px IAs and b) CFD simulation.

The circulation inside the drop changes during drop formation and a method of measuring this is to determine the angular velocity, which is a measure of the rotation of a fluid element as it moves in the flow field. The mean angular velocity around the z-axis in the centre cross section of the whole drop after 0.18 s was calculated to 25 s^{-1} with the data from the PIV experimental (Fig. 4a) and 26 s^{-1} with the data from the CFD simulation (Fig. 4b) at this early stage of the drop formation. The angular velocity increased to 30 s^{-1} in the PIV image (Fig. 5a) and to 30.5 s^{-1} in the CFD simulated drop (Fig. 5b) after 0.63 s and decreased to 20.5 and 21 s^{-1} in the PIV image and simulated drop, respectively, at a late stage of drop formation (2.16 s) in Fig. 6. The values from the two methods can be considered to agree well with each other since there is an uncertainty in both measurement methods.

The variation in average angular velocity with time during simulation of the drop formation is shown in Fig. 7. The angular velocity increases during the first fourth of the drop formation time since the drop is relatively small when the influence of the cross-flow starts to affect the drop. In addition, at the beginning of drop formation, the oil flux from the capillary influences the motion in the drop, thus affecting the amplitude of the angular velocity. As the drop continues to grow the influence of the cross-flow will increase, but since the drop radius also increases the net result will be a decrease in the average angular velocity. A steady state is approached as the point of drop detachment approaches, which indicates that the shear resulting from the cross-flow has a greater effect than during the decreasing angular velocity phase. The spread of the data during the early part of the simulated drop formation is mainly due to the location of the interface of the drop in relation to the grid cells. This problem is more pronounced when the drop is small and the number of cells occupied by the dispersed phase is limited.

The internal rotation may have a minor influence on drop detachment, but not as great as the influence from the drag from the cross-flow and the pressure around the drop. However, the analysis of angular velocity provides insight into the fluid transport within drops, which is important for mixing efficiency when the dispersed phase consists of an emulsion or several components, for example, surfactants or an active substance.

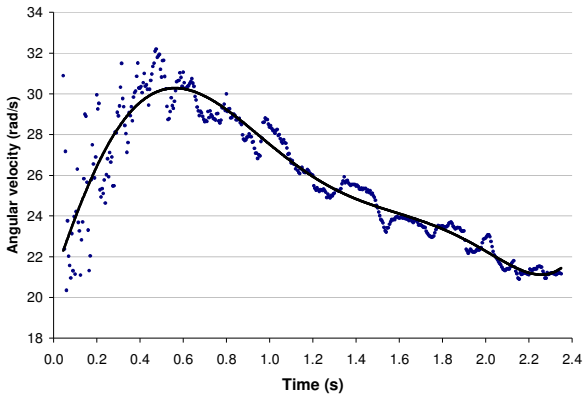

Fig. 7. Average angular velocity in the forming oil drop, which detaches at t=2.25 s

In both the PIV experiment and the numerical simulation a constant pressure was applied to the oil phase. However, this does not lead to a constant velocity of oil out of the capillary as can be seen in Fig. 8, which shows the simulated variation of the velocity out from the capillary and the pressure inside the centre of the forming drop with time. The pressure in the drop corresponds to the Laplace pressure, which is inversely proportional to the radius of a drop curvature. This results in a large pressure at the beginning of the drop formation process, and also at the end when the neck has been formed. The capillary velocity is not only affected by the constant pressure applied to the oil phase, but also by the pressure caused by the cross-flow above the capillary opening and, above all, by the pressure inside the drop.

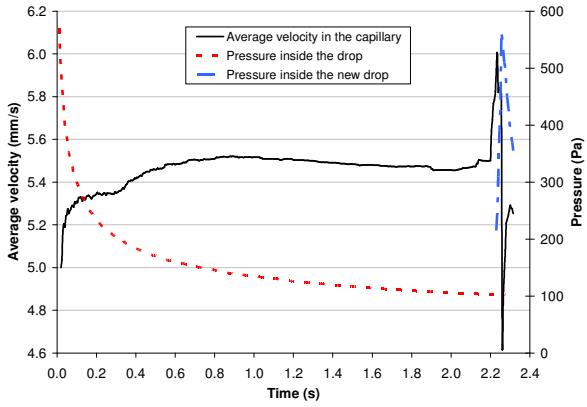

Fig. 8. Average velocity in the oil at the capillary opening and the pressure inside the forming drop during numerical simulation. Drop detachment occurs at t=0 and t=2.25 s

The maximum velocity in the capillary was observed just before the neck was formed, when the curvature of the drop interface was at a maximum. The oil phase had a minimum velocity in connection with detachment. Immediately before detachment the amount of oil between the neck and the capillary opening was small. In addition, this fraction of the oil was deformed, thus indicating that the radius could be assumed to be very small and therefore also result in a large pressure. The velocity increases again after detachment as an effect of the reorientation of the oil remaining at the capillary opening. The remaining deformed oil rest returns to a hemispherical shape, which decreases the pressure and increases the flow of oil out of the capillary. As the new drop grows the pressure will further decrease and hence the capillary velocity will increase. This

indicates that the pressure inside the forming drop has the largest effect on the velocity variations in the oil phase. Abrahamse et al. (2001) presented similar results, when they used a pore diameter of 5 µm in their simulations.

4 Conclusions

The experimental and computed data showed that the laminar continuous cross-flow and the jet from the capillary induce an internal rotational velocity in the forming oil drop. The experimental results have been compared to a numerical simulation of the drop formation process and the flow behaviour inside the forming drop and values of the angular velocity show a good agreement. The angular velocity approaches a steady state before drop detachment, when a neck is formed above the capillary opening. The numerical simulation shows further that the pressure inside the forming drop affects the velocity of oil leaving the capillary. A high internal pressure causes a decreased average velocity at the capillary opening. The PIV method can, together with numerical simulations, be used to show valuable physical phenomena, which will improve the knowledge of the drop formation and detachment process.

Acknowledgement

This work was financially supported by the Swedish Research Council.

References

Abrahamse AJ, van der Padt A, Boom RM, de Heij WBC (2001) Process fundamentals of membrane emulsification: Simulation with CFD. AIChE J 47:1285-1291
Antar MA, El-Shaarawi MAI (2002a) Effect of viscosity ratio, spin and Reynolds number on the flow characteristics about a liquid sphere in a gas stream. Int J Num Meth Heat Fluid Flow 12:800-816
Antar MA, El-Shaarawi MAI (2002b) Mixed convection around a liquid sphere in an air stream. Heat Mass Transfer 38:419-424
Antar MA, El-Shaarawi MAI (2004) Simultaneous effect of rotation and natural convection on the flow about a liquid sphere. Heat Mass Transfer 40:393-399
Augier F, Masbernat O, Guiraud P (2003) Slip velocity and drag law in a liquid-liquid homogeneous dispersed flow. AIChE J 49:2300-2316
Crowe CT, Sommerfeld M, Tsuji Y (1998) Multiphase flows with droplets and particles. p.24, New York: CRC press
Hill MJM (1894) On a spherical vortex. Phil Trans R Soc 185:213-245
Joscelyne SM, Trägårdh G (1999) Food emulsions using membrane emulsification: conditions for producing small droplets. J Food Eng 39:59-64
Kobayashi I, Yasuno M, Iwamoto S, Shono A, Satoh K, Nakajima M (2002) Microscopic observation of emulsion droplet formation from a polycarbonate membrane. Coll Surf Physicochem Eng Aspects 207:195-196
Kobayashi I, Mukataka S, Nakayima M (2004) CFD simulation and analysis of emulsion droplet formation from straight-through microchannels. Langmuir 20:9868-9877
Kobayashi I, Uemura K, Nakajima M (2006) CFD study of the effect of a fluid flow in a channel on generation of oil-in-water emulsion droplets in a straight-through microchannel emulsification. J Chem Eng Japan 39:855-863
Megaridis CM, Hodges JT, Xin J, Day JM, Presser C (1994) Internal droplet circulation induced by surface-driven rotation. Int J Heat Fluid Flow 15:364-377
Mohamed-Kassim Z, Longmire EK (2003) Drop impact on a liquid-liquid interface. Phys Fluids 15:3263-3273
Mohamed-Kassim Z, Longmire EK (2004) Drop coalescence through a liquid/liquid interface. Phys Fluids 16:2170-2181
Milosevic IN, Longmire EK (2002) Pinch-off modes and satellite formation in liquid/liquid jet systems. Int J Multiphase Flow 28:1853-1869

Ohta M, Yamamoto M, Suzuki M (1995) Numerical analysis of a single drop formation process under pressure pulse conditions. Chem Eng Sci 50:2923-2931
Ohta M, Iwasaki A, Obata E, Yoshida Y (2003) A numerical study of the motion of a spherical drop rising in shear-thinning fluid systems. J Non-Newtonian Fluid Mech 116:95-111
Rayner M, Trägårdh G, Trägårdh C, Dejmek P (2004) Using the Surface Evolver to model droplet formation processes in membrane emulsification. J Colloid Interface Sci 279:175-185
Schröder V, Behrend O, Schubert H (1998) Effect of dynamic interfacial tension on the emulsification process using microporous, ceramic membranes. J Colloid Interface Sci 202:334-340
Schönfeld F, Rensink D (2003) Simulation of droplet generation by mixing nozzles. Chem Eng Tech 26:585-591
Sugiura S, Nakajima M, Iwamoto S, Seki M (2001) Interfacial tension driven monodispersed droplet formation from microfabricated channel array. Langmuir 17:5562-5566
Timgren A, Trägårdh G, Trägårdh C Application of the PIV technique to measurements around and inside a forming drop in a liquid-liquid system. Manuscript
Timgren A, Trägårdh G, Trägårdh C (2007) CFD modelling of drop formation in a liquid-liquid system. In: Proceedings of the 6th International Conference on Multiphase Flow, Leipzig, Germany, July 9-13
Wang Z, Wang S, Schröder V, Schubert H (2000) Effect of continuous phase viscosity on membrane emulsification. Chinese J Chem Eng 8:108-112
Westerweel J (1993) Particle image velocimetry – Theory and application. Ph.D Thesis. Delft University Press
Westerweel J (2000) Theoretical analysis of the measurement precision in particle image velocimetry. Exp Fluids [Suppl.] S3-S12
Yasuno M, Nakajima M, Iwamoto S, Maruyama T, Sugiura S, Kobayashi I, Shono A, Satoh K (2002) Visualization and characterization of SPG membrane emulsification. J Membr Sci 210:29-37